



AMS
American Meteorological Society

Supplemental Material

Journal of Climate

Isolating the Evolving Contributions of Anthropogenic Aerosols and Greenhouse Gases: A New
CESM1 Large Ensemble Community Resource
<https://doi.org/10.1175/JCLI-D-20-0123.1>

[© Copyright 2020 American Meteorological Society](#)

Permission to use figures, tables, and brief excerpts from this work in scientific and educational works is hereby granted provided that the source is acknowledged. Any use of material in this work that is determined to be “fair use” under Section 107 of the U.S. Copyright Act or that satisfies the conditions specified in Section 108 of the U.S. Copyright Act (17 USC §108) does not require the AMS’s permission. Republication, systematic reproduction, posting in electronic form, such as on a website or in a searchable database, or other uses of this material, except as exempted by the above statement, requires written permission or a license from the AMS. All AMS journals and monograph publications are registered with the Copyright Clearance Center (<http://www.copyright.com>). Questions about permission to use materials for which AMS holds the copyright can also be directed to permissions@ametsoc.org. Additional details are provided in the AMS Copyright Policy statement, available on the AMS website (<http://www.ametsoc.org/CopyrightInformation>).

SUPPLEMENTAL MATERIALS

Isolating the Evolving Contributions of Anthropogenic Aerosols and Greenhouse Gases from Internal Variability: A New CESM1 Large Ensemble Community Resource

Clara Deser^{*}, Adam S. Phillips, Isla R. Simpson, Nan Rosenbloom, Dani Coleman,

Flavio Lehner and Angeline G. Pendergrass

Climate and Global Dynamics Division, NCAR, Boulder CO

Pedro DiNezio

University of Texas at Austin

Samantha Stevenson

University of California at Santa Barbara

Submitted to *Journal of Climate*

23 February 2020

Revised 25 June 2020

** Corresponding author: Dr. Clara Deser (cdeser@ucar.edu)*

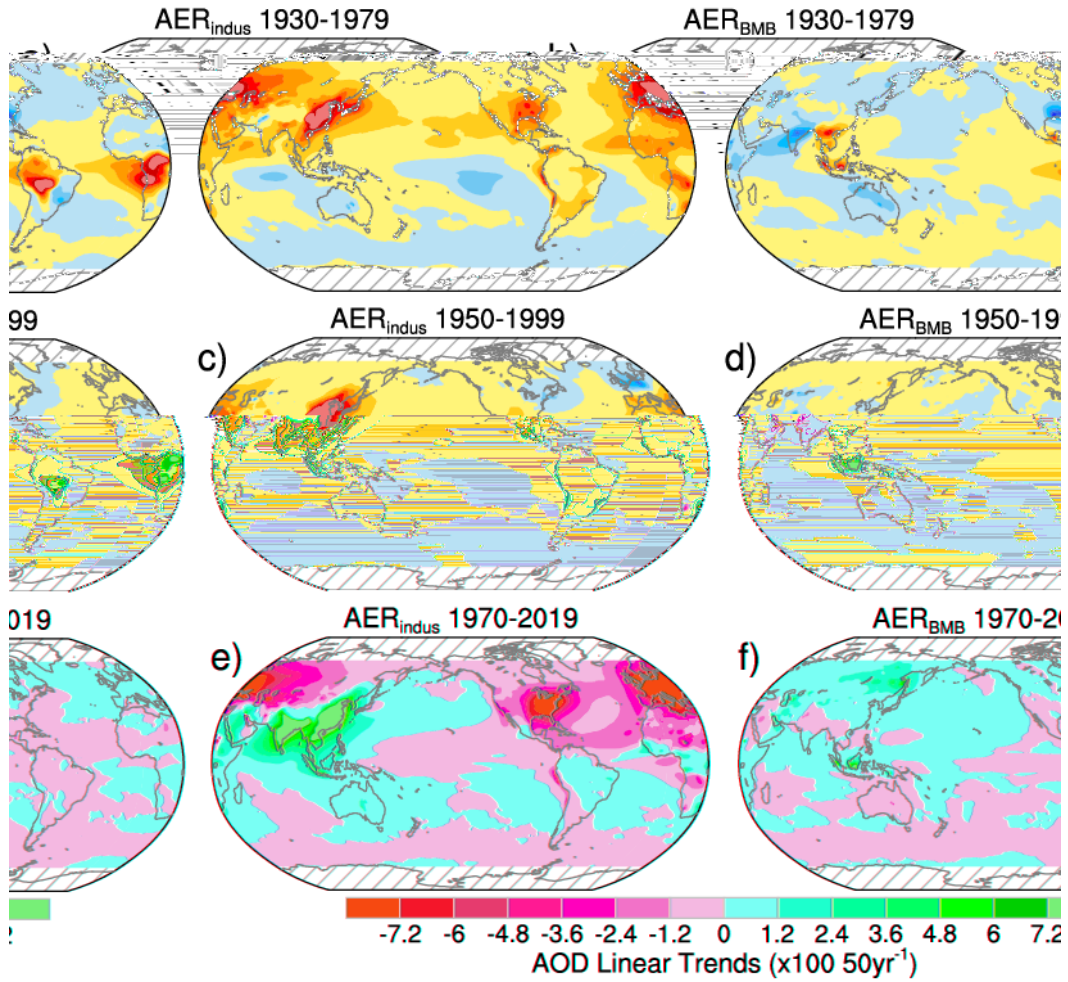


Figure S1. Linear trends in ensemble-mean Aerosol Optical Depth (AOD) at a wavelength of 550nm (per 50 years, multiplied by 100) for: a) AER_{indus} 1930-1979; b) AER_{indus} 1950-1999; and d) AER_{indus} 1970-2019; e) AER_{bmb} 1930-1979; f) AER_{bmb} 1950-1999; and g) AER_{bmb} 1970-2019. AER_{indus} denotes the industrial aerosol ensemble and AER_{bmb} denotes the biomass burning aerosol ensemble. AOD values in polar regions (hatching) are omitted for plotting purposes only.

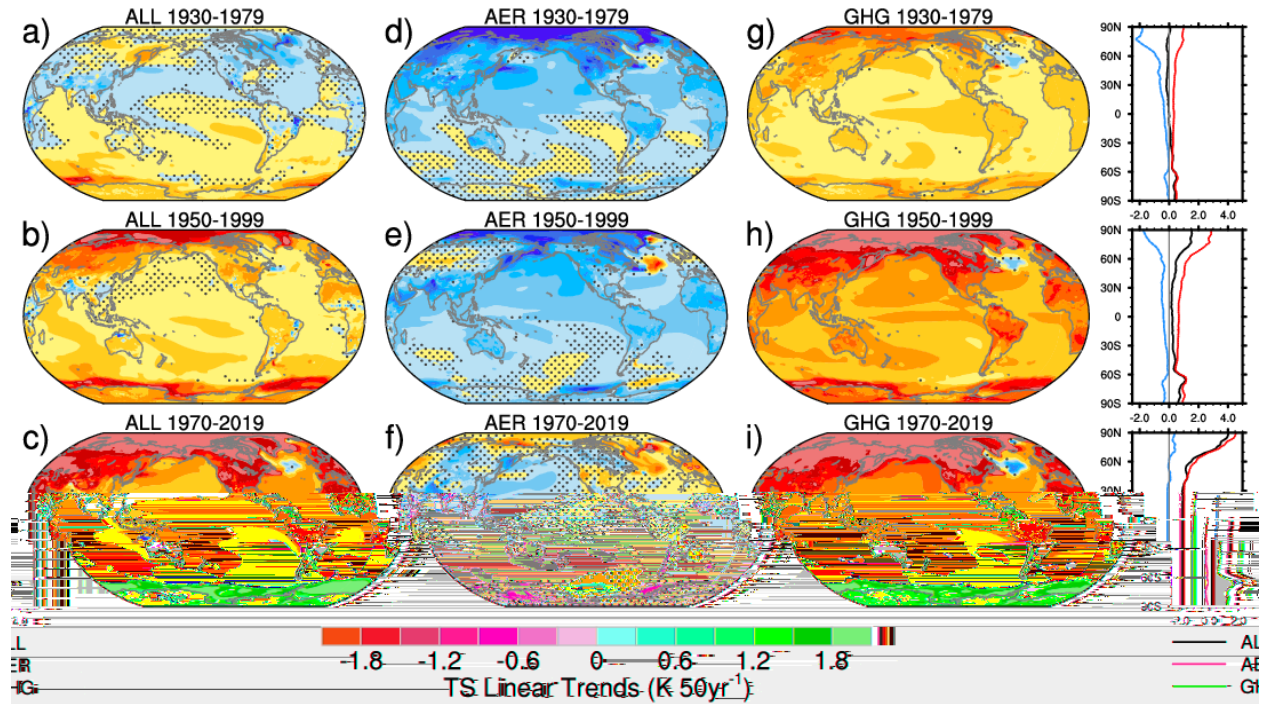


Figure S2. Linear trends in CESM1 ensemble-mean surface temperature (TS; K per 50 years) based on: a) ALL 1930-1979; b) ALL 1950-1999; c) ALL 1970-2019; d) AER 1930-1979; e) AER 1950-1999; f) AER 1970-2019; g) GHG 1930-1979; h) GHG 1950-1999; i) GHG 1970-2019. Stippled regions indicate insignificant values at the 90% confidence level based on a 2-sided t-test. Panels on the right show zonal-mean profiles of the trend maps in each row: ALL (black), AER (blue) and GHG (red).

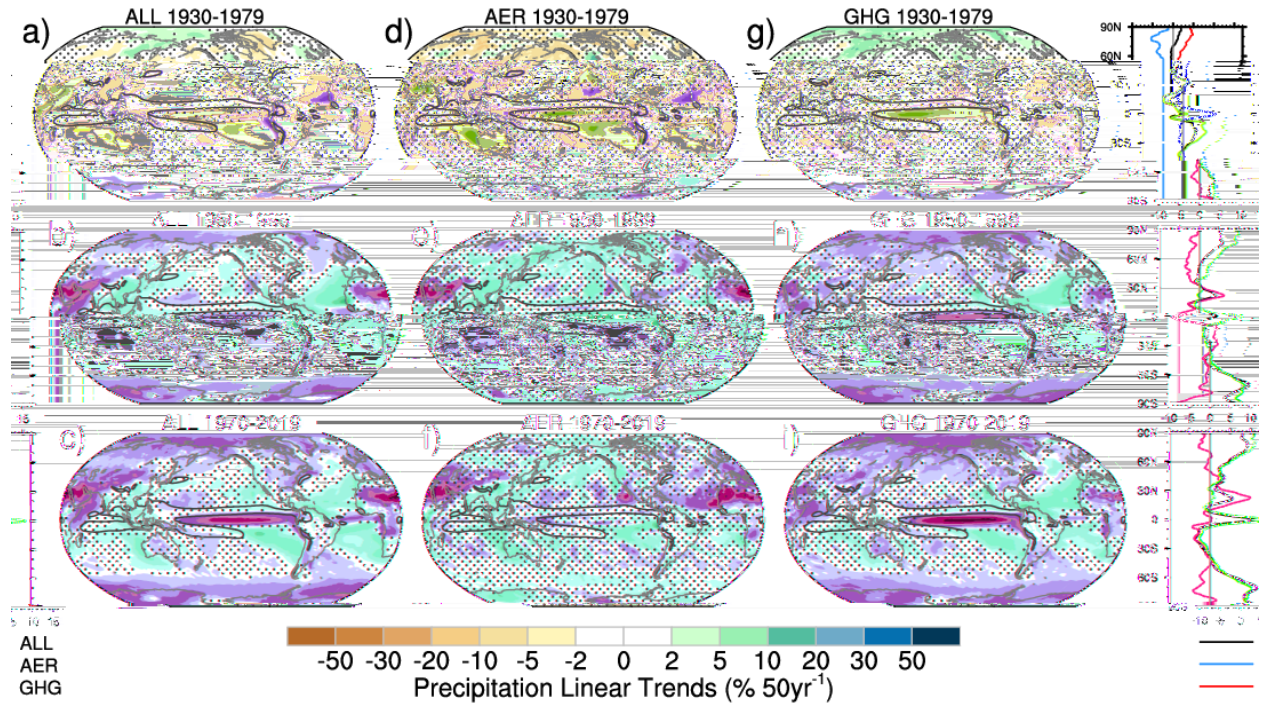


Figure S3. Linear trends in CESM1 ensemble-mean precipitation expressed as a percentage of the ensemble-mean ALL climatology in each period (% per 50 years) for: a) ALL 1930-1979; b) ALL 1950-1999; c) ALL 1970-2019; d) AER 1930-1979; e) AER 1950-1999; f) AER 1970-2019; g) GHG 1930-1979; h) GHG 1950-1999; i) GHG 1970-2019. Stippled regions indicate insignificant values at the 90% confidence level based on a 2-sided t-test. The contours show the 6 mm/day isopleth of the precipitation climatology. Panels on the right show zonal-mean profiles of the trend maps in each row (i.e., zonal means of the % trends at each grid box): ALL (black), AER (blue) and GHG (red).

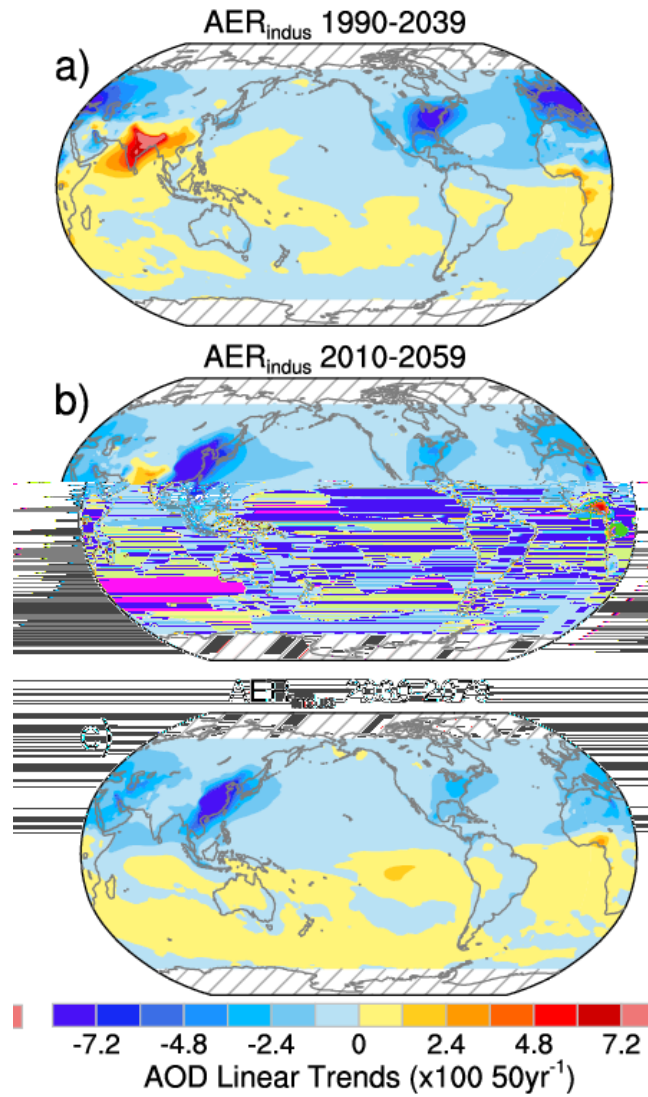


Figure S4. Linear trends in ensemble-mean Aerosol Optical Depth (AOD) at a wavelength of 550nm (per 50 years, multiplied by 100) from AERindus for: a) 1990-2039; b) 2010-2059; and c) 2030-2079. AOD values in polar regions (hatching) are omitted for plotting purposes only.

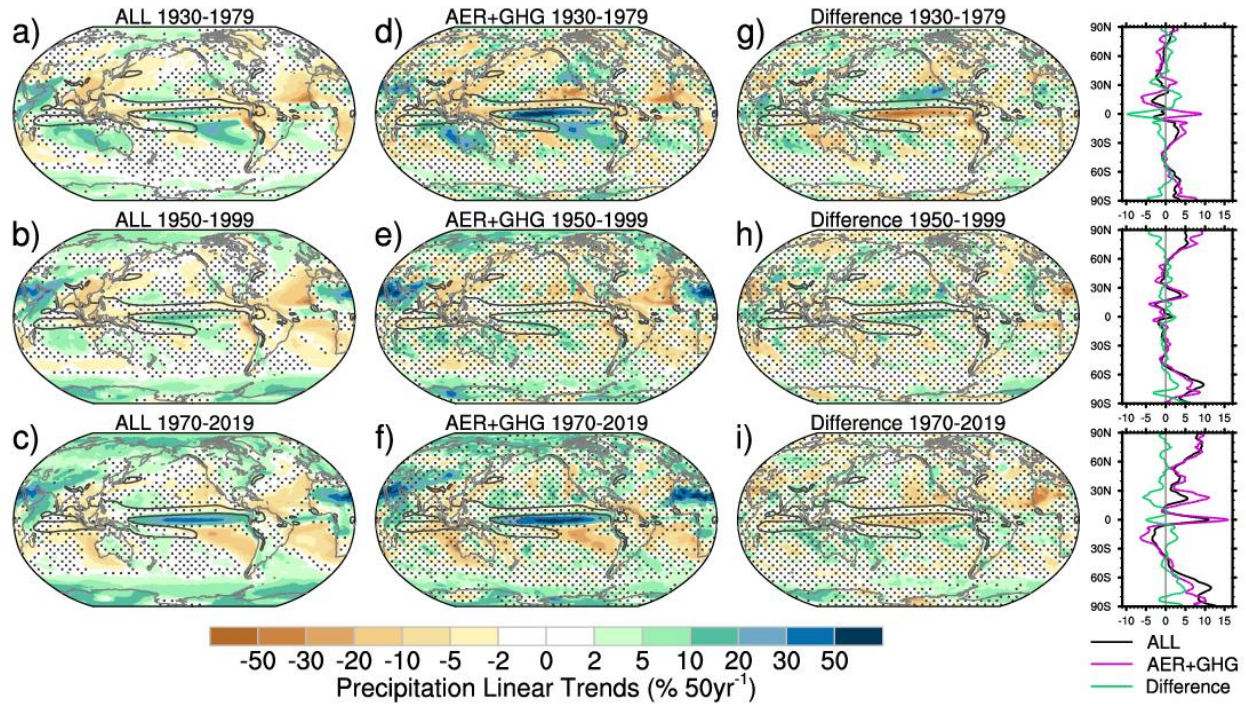


Figure S5. Linear trends in CESM1 ensemble-mean precipitation expressed as a percentage of the ensemble-mean ALL climatology in each period (% per 50 years) for: a) ALL 1930-1979; b) ALL 1950-1999; c) ALL 1970-2019; d) AER+GHG 1930-1979; e) AER+GHG 1950-1999; f) AER+GHG 1970-2019; g) ALL minus AER+GHG 1930-1979; h) ALL minus AER+GHG 1950-1999; i) ALL minus AER+GHG 1970-2019. Stippled regions indicate insignificant values at the 90% confidence level based on a 2-sided t-test. The contours show the 6 mm/day isopleth of the precipitation climatology. Panels on the right show zonal-mean profiles of the trend maps in each row (i.e., zonal means of the % trends at each grid box): ALL (black), AER+GHG (purple) and their difference (green).

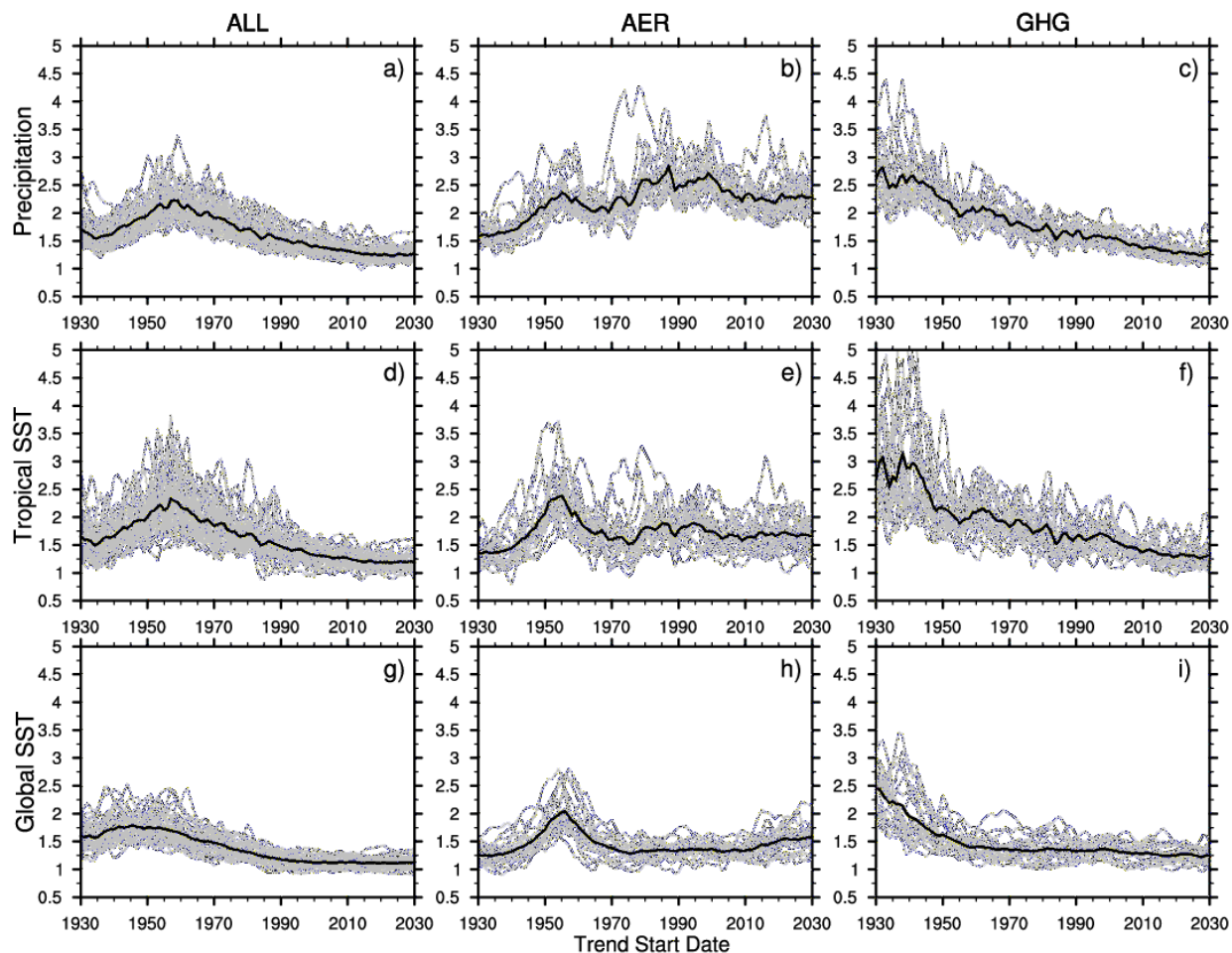


Figure S6. (Gray curves) Spatial RMS of running 50-year trends from each individual ensemble member relative to the ensemble-mean of: a) ALL tropical precipitation; b) AER tropical precipitation; c) GHG tropical precipitation; d) ALL tropical SST*; e) AER tropical SST*; f) GHG tropical SST*; g) ALL global SST*; h) AER global SST*; and i) GHG global SST*. The asterisk denotes that the domain-mean SST trend has been removed before computing the spatial RMS. Thick black curves are the average of the gray curves. The time axis denotes the start year of each 50-year trend. Results for global precipitation are nearly identical to those for tropical precipitation.

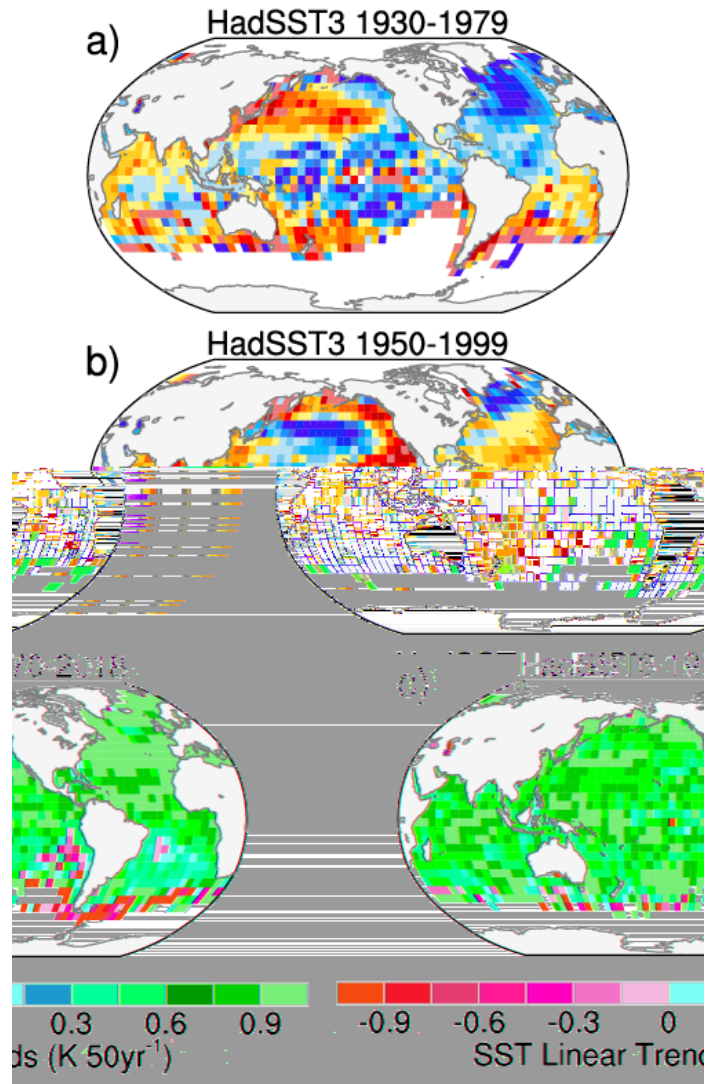


Figure S7. Linear SST trends from HadSST3 (K per 50 years) during: a) 1930-1979; b) 1950-1999; c) 1970-2018. White areas denote missing data.

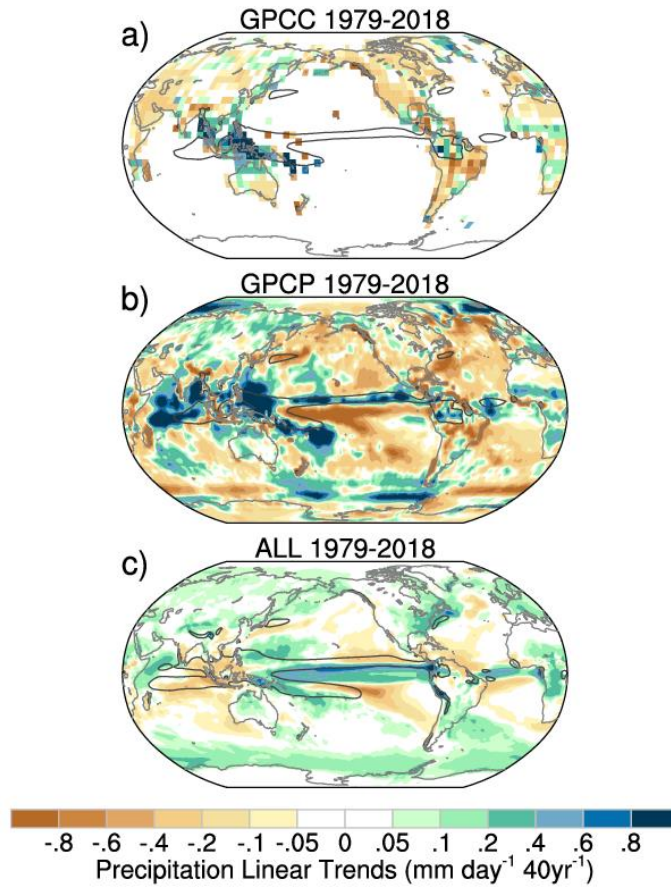


Figure S8. Linear precipitation trends (mm/day per 50 years) during 1979-2018 from: a) GPCP; b) GPCP; and c) ALL ensemble-mean. White areas over ocean in panel a) denote missing data.